



## Low-temperature thermal properties and features of the phonon spectrum of lutetium tetraboride



V.V. Novikov<sup>a</sup>, N.V. Mitroshenkov<sup>a,\*</sup>, A.V. Matovnikov<sup>a</sup>, D.V. Avdashchenko<sup>a</sup>, A.V. Morozov<sup>b</sup>, L.M. Pavlova<sup>c</sup>, V.B. Koltsov<sup>c</sup>

<sup>a</sup>Bryansk Petrovsky State University, 14 Bezhitskaya St., Bryansk 241037, Russia,

<sup>b</sup>Russian Timiryazev State Agrarian University, 49 Timiryazevskaya St., Moscow 127550, Russia

<sup>c</sup>National Research University of Electronic Technology "MIET", Moscow 124498, Russia

### ARTICLE INFO

#### Article history:

Received 7 May 2014

Received in revised form 5 June 2014

Accepted 5 June 2014

Available online 14 June 2014

#### Keywords:

Rare earth alloys and compounds

Heat capacity

Thermal expansion

Thermal analysis

### ABSTRACT

The coefficients of thermal expansion to the *c* axis ( $\alpha_{\parallel}$ ,  $\alpha_{\perp}$ ) were measured for lutetium tetraboride over the temperature range 4.2–300 K. The heat capacity data for lutetium tetraboride were used for the calculation of tetraboride phonon spectrum moments and also for the development of a simplified tetraboride spectrum model. The use of the heat capacity and thermal expansion data allowed the temperature changes of the Grüneisen parameters  $\Gamma$ ,  $\Gamma_{\parallel}$ ,  $\Gamma_{\perp}$  for tetraboride to be calculated.

As a result of the approximation of  $\Gamma_{\perp}(T)$ ,  $\Gamma_{\parallel}(T)$  temperature dependencies in accordance with the chosen phonon spectrum model have been found: the anomalies of  $\Gamma_{\perp}(T)$ ,  $\Gamma_{\parallel}(T)$  are at about 25 K and then drop at lower temperatures due to the Einstein vibrations of boron sublattices.

© 2014 Published by Elsevier B.V.

### 1. Introduction

Tetraborides of rare-earth elements (RB<sub>4</sub> compounds, in which R stands for the rare-earth element), in addition to the high hardness and melting temperature typical of all rare-earth borides, also possess a number of properties making them rather interesting from the general scientific and practical perspectives. The application-oriented interest in rare-earth tetraborides is primarily conditioned by the magnetic and structural transformations occurring in most of them [1–10]. As a result of these transformations, a number of physical and thermodynamic characteristics change in discrete steps. Such changes in their properties can be used for producing various switching devices, magnetic cooling devices and so forth [11]. Of great theoretical interest is the research of the ordering processes in the tetraborides' magnetic sub-systems, which are, on the one hand, conditioned by the characteristic properties of R<sup>3+</sup> paramagnetic ions and, on the other hand, by the peculiarity of their spatial location caused by the unique crystalline structure of RB<sub>4</sub> compounds.

Tetraborides of rare-earth elements are characterized by the tetragonal crystalline structure of the UB<sub>4</sub> type,  $D_{2h}^5 - P4/mbm$ . The unit cell contains four formula units [12].

Boron sub-lattice is made up of B<sub>6</sub> octahedra (the structural unit of the boron sub-lattice of rare-earth hexaborides), connected by chains of boron atoms, which, together with the octahedron ribs, form the distorted heptangular rings. This ring-shaped arrangement of boron atoms is characteristic of rare-earth diborides. A tetraboride lattice is represented as alternate layers of metal and boron atoms (Fig. 1) [13].

Above the rings of boron atoms there are metal atoms which form squares and triangles in the plane perpendicular to the crystal *c* axis. This mutual arrangement of R<sup>3+</sup> paramagnetic ions corresponds to the so-called Shastry–Sutherland lattice (SSL), the most characteristic feature of which is a geometric frustration, that is the impossibility of complete ordering in the system of atomic magnetic moments up to the absolute zero [14] and, as a consequence, the presence of zero-point entropy [15–17].

For the successful study of the features of electronic and magnetic sub-systems of the magnetic materials, it is often necessary to single out the influence of the phonon sub-system on the values of the properties under study. To evaluate the lattice contribution to the characteristics of magnetic materials, the method of comparison with the non-magnetic isostructural analogue is usually employed. For the family of rare-earth tetraborides these diamagnetic analogues are lanthanum and lutetium tetraborides (LaB<sub>4</sub> and LuB<sub>4</sub> respectively).

As follows from the phase diagrams and our experiments, it is much more difficult to synthesize the single-phased sample of

\* Corresponding author.

E-mail addresses: [vvnovikov@mail.ru](mailto:vvnovikov@mail.ru) (V.V. Novikov), [weerm@yandex.ru](mailto:weerm@yandex.ru) (N.V. Mitroshenkov).

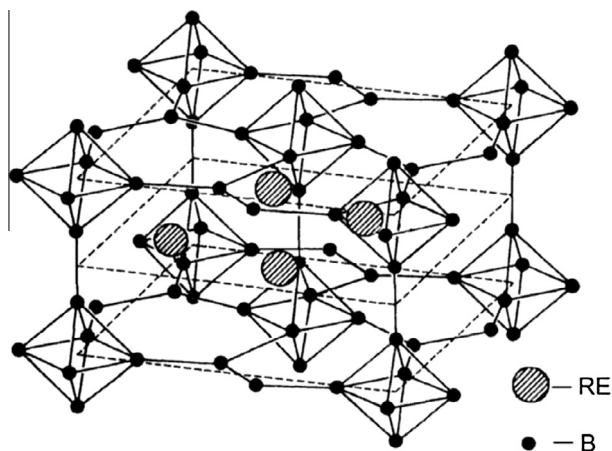
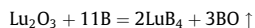


Fig. 1. The unit cell of  $RB_4$ .

lanthanum tetraboride than lutetium tetraboride. Therefore, to study the phonon properties of rare-earth tetraborides at low temperatures, the lutetium tetraboride was chosen ( $LuB_4$ ).

## 2. Experiment

The polycrystalline sample of lutetium tetraboride was synthesized by the method of boron-thermal reduction of metal from its oxide in a vacuum [17]:



For the synthesis we used lutetium oxide of 99.9% purity produced by Mosreaktiv, as well as the elemental boron of 99% purity produced by ErmakKhim. The synthesis was carried out in the vacuum electric furnace manufactured by Termotekhnik ML. At the first stage of synthesis, we annealed the stoichiometric mixture of oxide and boron at a temperature of  $T_1 = 1473$  K for 3 h at a pressure of  $10^{-1}$  Pa. The X-ray diffraction pattern of the synthesized sample obtained by the X-ray diffractometer DRON-7 (Burevestnik Research and Manufacturing Association) in  $Co K\alpha$  radiation was compared to the ASTM data and contained the reflections of tetraboride, oxide and metal phases (Fig. 2a). To eliminate the excess phases, the sample, previously comminuted to a powdery condition and then compacted into a tablet, underwent additional annealing at a temperature of  $T_1 = 1973$  K for 1 h. After the second annealing, the X-ray diffraction pattern contained the reflexes of the only phase – the  $LuB_4$  phase (Fig. 2b). According to the chemical analysis, the synthesized sample contains 19.74% lutetium, and 80.27% boron. The crystalline lattice parameters for the  $LuB_4$  sample were as follows:  $a = 0.70336$  nm,  $c = 0.39732$  nm (according to [12]  $a = 0.7036$  nm,  $c = 0.3974$  nm).

The  $a$  and  $c$  lattice parameters for lutetium tetraboride in the temperature range of 5–300 K were determined by the Debye–Scherrer method using the X-ray diffractometer DRON-7.0 in  $Co K\alpha$  radiation with Bragg–Bretanno focusing. From the synthesized  $LuB_4$  powder, a tablet 13 mm in diameter and 1 mm thick was formed by means of pressing with a small amount of an organic binding agent. The tablet was placed in the copper cuvette of the X-ray helium cryostat, which was equipped with a constantan wire heater 0.05 mm thick. The signal from the ‘Constantan–Copper +0.1% Iron’ thermocouple, whose junction point was adjusted to the copper

cuvette, reached the temperature regulator which kept the cuvette temperature in the range of 5–300 K with an accuracy of not less than 0.05 K. To find the values for the  $a$  and  $c$  lattice parameters of lutetium tetraboride we experimentally worked out the angle positions for  $\theta$  Bragg reflections (214) and (271) at room temperature:  $2\theta_{214} = 141.6^\circ$  and  $2\theta_{271} = 144.6^\circ$ . These reflections belong to the high-angle region of scattering and are well-represented. At room temperature, the Bragg angles of scattering for 28 reflexes were evaluated. Then the  $a_{hkl}(\cos^2 \theta_{hkl})$ ,  $c_{hkl}(\cos^2 \theta_{hkl})$  dependencies were calculated, which were extrapolated to zero. The ordinate intersection of  $a_{tr}(300\text{ K}) = 0.70336$  nm,  $c_{tr}(300\text{ K}) = 0.39732$  nm were considered the true values of the  $a$  and  $c$  parameters for lutetium tetraboride at room temperature. Differences  $\Delta a = a_{tr}(300\text{ K}) - a_{\theta_1, \theta_2}(300\text{ K})$ ,  $\Delta c = c_{tr}(300\text{ K}) - c_{\theta_1, \theta_2}(300\text{ K})$  were considered as constant values within the whole temperature range and were used as corrections to the values of  $a_{\theta_1, \theta_2}(T)$ ,  $c_{\theta_1, \theta_2}(T)$ . Here  $\theta_1, \theta_2$  are the reflex scattering angles (214) and (271), respectively, within the range of 4.2–300 K.

The heat capacity of the  $LuB_4$  sample in the range of 2–300 K was measured in the adiabatic vacuum calorimeter produced by Termax, the construction of which is similar to the one described above [18]. The sample temperature in the process of the calorimetric experiment was measured using a ferrous-rhodium thermometer with an accuracy of  $\pm 0.05$  K. The experimental adiabatic conditions were automatically maintained. In each heating cycle, the sample temperature increased by 0.2–0.5 K. The inaccuracy of the heat capacity evaluation amounted to 3% at 2–20 K. At 60 K it decreased to 1% and remained within this range up to the room temperatures. The difference in the calibration measurement results of the sample of electrolytic copper, annealed and melted in the vacuum, from the recommended values [19] did not exceed the inaccuracy indicated above.

## 3. Results and discussion

In Table 1, one can see the smoothed values of  $C_p(T)$   $LuB_4$  molar heat capacity in the temperature range under study. Fig. 2a and b illustrate the experimental dependencies of  $C_p(T)$ ,  $C_p/T^3(T^2)$ .  $C_p(T)$  dependency (Fig. 2a) has the features typical of diamagnetic rare-earth borides within the range of low temperatures [20]. One can clearly see the smooth anomaly of the  $C_p(T)$  curve within the range of 25–75 K and the dependency close to the linear at the higher temperatures (100–300 K). The bell-shaped maximum at the dependency  $C_p/T^3(T^2)$  (Fig. 2b) signals the presence of Einstein components for  $LuB_4$  heat capacity. The increase in the  $C_p/T^3(T^2)$  curve is conditioned by the contribution of the electron gas into the boride heat capacity:  $C_{el} = 0.00017$  J/g at K.

We approximated the phonon spectrum of lutetium tetraboride by the following expression:

$$G(\omega) = a_1\omega^3 + a_2\omega^3 + a_3\delta(\omega - \omega_{1E}) + a_4\delta(\omega - \omega_{2E}),$$

$$\omega < \omega_{1\max} \quad \omega < \omega_{2\max} \quad (1)$$

where  $a_1, a_2$  are determined from the values of the characteristic Debye temperatures of  $\theta_{1D}, \theta_{2D}$ ; and  $\omega_{1m}, \omega_{2m}$  are frequencies at which Debye parabolic phonon spectra are cropped. The values of these spectra as well as the  $a_3, a_4$  coefficients, were chosen for the best correspondence to the experimental data.

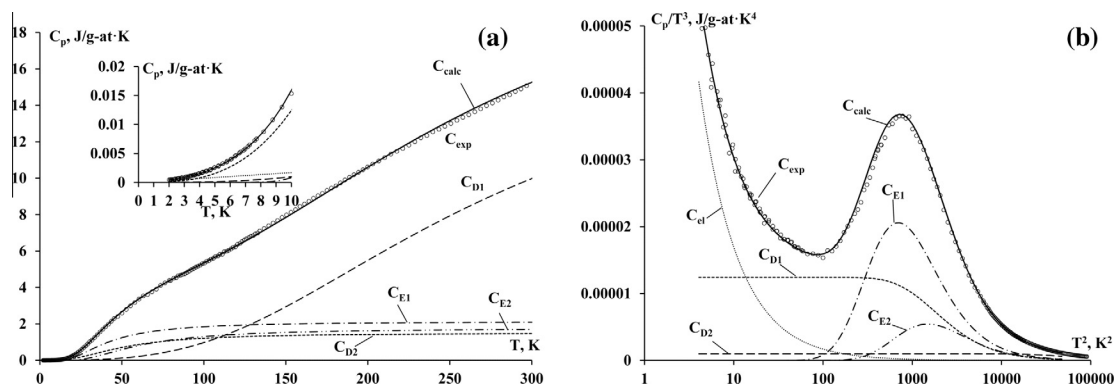


Fig. 2. Lutetium tetraboride heat capacity (a)  $C_p(T)$  dependency and (b)  $C_p/T^3(T^2)$  dependency.

Download English Version:

<https://daneshyari.com/en/article/1610647>

Download Persian Version:

<https://daneshyari.com/article/1610647>

[Daneshyari.com](https://daneshyari.com)